Micro-Raman study and phase transitions of $Nd_{0.5}Ca_{0.5}MnO_3$

2006 J. Phys.: Condens. Matter 18 1667

(http://iopscience.iop.org/0953-8984/18/5/019)

INSTITUTE OF PHYSICS PUBLISHING JOURNAL OF PHYSICS: CONDENSED MATTER

J. Phys.: Condens. Matter **18** (2006) 1667–1676 doi:10.1088/0953-8984/18/5/019

Micro-Raman study and phase transitions of $Nd_{0.5}Ca_{0.5}MnO_3$

S Jandl[1], A A Mukhin[2], V Yu Ivanov[2] and A M Balbashov[3]

[1] Département de Physique, Université de Sherbrooke, Sherbrooke, QC, J1K2R1, Canada
[2] General Physics Institute of the Russian Academy of Sciences, 38 Vavilov Street, 119991 Moscow, Russia
[3] Moscow Power Engineering Institute, 14 Krasnokazarmennaya Street, 105835 Moscow, Russia

Received 28 October 2005, in final form 22 December 2005
Published 18 January 2006
Online at stacks.iop.org/JPhysCM/18/1667

Abstract

A micro-Raman study of high quality $Nd_{0.5}Ca_{0.5}MnO_3$ single crystals is presented, with temperature variation. Twelve A_g and eight B_{2g} Raman active modes (simplified symmetry: *Pmma* space group) have been observed in resonance conditions and compared to the parent and charge ordered compound phonons.

The detected $Nd_{0.5}Ca_{0.5}MnO_3$ phonons retrace the magnetic and structural temperature evolutions in the paramagnetic, charge ordered ($T_{co} \sim 250$ K) and antiferromagnetic orbital ordered ($T_N \sim 160$ K) regimes. In particular, at $T < T_N$, phase separation and also rotational and coherent Jahn–Teller MnO_6 distortions prevail.

1. Introduction

Replacement of the rare earth ion R^{3+} by a divalent cation A^{2+} generates Mn^{4+} ions in $R_{1-x}A_xMnO_3$ (R = lanthanides and A = Ba, Sr, or Ca) leading to double-exchange interactions and reduction of Jahn–Teller-type distortions [1–3]. Governed by the amount of doping and the tolerance factor [4], the temperature dependent electric characters of doped manganites evolve into paramagnetic insulator, ferromagnetic metallic and charge ordered insulator states. Near either the concomitant paramagnetic insulator–ferromagnetic metallic phase transition [5] or the ferromagnetic metallic–charge ordered insulator transition [6], a colossal negative magnetoresistance, reflecting strong interconnections between the electrical and magnetic properties, is observed. As a function of temperature and doping, the Mn^{3+}/Mn^{4+} distribution modifies the Mn–O–Mn bond length and angle and provokes structural disorder. The charge transfer from an occupied Mn^{3+} e_g orbital to an adjacent Mn^{4+} unoccupied e_g orbital depends strongly on the MnO_6 octahedra tiltings and Jahn–Teller distortions. Also, in such doped compounds, whether doping at different levels results in homogeneous or coexisting phases remains an important issue for theoretical modelling centred on phase separation [7]. In

particular, it was found that electron rich ferromagnetic and electron poor antiferromagnetic domains can occur in charge ordered phases [8].

At low temperatures, the strongly doped manganites ($x \sim 0.5$) become insulating with the decrease of the R^{3+} and A^{2+} radii and the corresponding formation of charge and orbital ordering as well as CE-type antiferromagnetism [9]. The transition from a ferromagnetic metallic phase to an antiferromagnetic insulating charge–orbital ordered phase was first observed in $La_{0.5}Ca_{0.5}MnO_3$. At temperatures below 150 K a superstructure (space group $P2_1/m$) with double the a lattice parameter of $LaMnO_3$ ($Pnma$ unit cell) is formed [10]. The charge ordering develops in the ac planes where each Jahn–Teller distorted $Mn^{3+}O_6$ octahedron is surrounded by four undistorted $Mn^{4+}O_6$ octahedra and vice versa. Rows of octahedra of one type are aligned along the b axis. Recent electron diffraction and dark field imaging for $La_{0.5}Ca_{0.5}MnO_3$ have shown that charge order exists in regions with no net magnetization and, surprisingly, can occur in ferromagnetic regions [11].

Compared to the La compounds, the Nd-based compounds have been less studied; they are nevertheless interesting since the strength of the double-exchange interactions is weaker due to larger lattice distortions provoked by the smaller Nd ions [12]. Consequently, in doped systems like $Nd_{1-x}(Ca, Sr)_xMnO_3$ as compared to $La_{1-x}(Ca, Sr)_xMnO_3$, closer competitions with new generic instabilities would exist between the electron–phonon, electron–electron and exchange interactions [13]. Phase separations may be expected in $Nd_{0.5}(Sr, Ca)_{0.5}MnO_3$, which are at the phase boundary separating the charge disordered A-type antiferromagnetic phase from the CE-type charge ordered phase [14]. Also the onsets of charge and orbital ordering in $Nd_{0.5}(Sr, Ca)_{0.5}MnO_3$ are accompanied by marked jumps in resistivity and magnetization [15, 16].

In $Nd_{0.5}Sr_{0.5}MnO_3$ the ferromagnetic metallic state develops at $T_c \sim 250$ K, extending down to $T_N \sim 150$ K, where the system becomes charge and orbital ordered, antiferromagnetic and insulating [17]. In contrast to $Nd_{0.5}Sr_{0.5}MnO_3$, $Nd_{0.5}Ca_{0.5}MnO_3$ which is characterized by the 1.17 Å weighted average radius of the Ca^{2+} cation as compared to 1.24 Å for the Sr^{2+} cation radius [9], charge ordering occurs at a much higher temperature than the antiferromagnetic order ($T_{co} \sim 250$ K as compared to $T_N \sim 160$ K). For $T_N < T < T_{co}$, while the magnetization and the susceptibility are typical of an antiferromagnet, no magnetic order is detected by means of neutron diffraction. Between room temperature and T_{co}, the tendency towards ferromagnetic order is disturbed by gradual charge ordering antiferromagnetism as confirmed by susceptibility measurements [18]. Nevertheless, ferromagnetic correlations are manifest in the charge disordered paramagnetic phase above T_{co}. In the intermediate temperature range $T_N < T < T_{co}$, charge ordering persists and orbital ordering sets in gradually until it is achieved around T_N, as suggested by the temperature variations of the lattice parameters [19]. Below T_N, with complete charge and orbital ordering, CE-type antiferromagnetism prevails [19, 20]. Also, in a recent Brillouin scattering study, Murugavel *et al* [21] have associated magnetic excitations in $Nd_{0.5}Ca_{0.5}MnO_3$ with ferromagnetic correlations down to 27 K indicating possible phase separation below T_{co}.

Raman spectroscopy has proved its efficiency in the characterization of the mixed valence manganite disorder with the detection of the oxygen partial phonon density of states and phase separation [22, 23]. Abrashev *et al* [24] have studied by Raman spectroscopy the charge and orbital ordered state in $La_{0.5}Ca_{0.5}MnO_3$. They observed that the new activated Raman modes, below $T \sim 150$ K, in the antiferromagnetic insulating ordered state were enhanced when excited with laser energies close to the Jahn–Teller gap ~1.9 eV. The most intense modes were assigned in comparison with layered manganites and undoped $RMnO_3$ (R = La, Y). $Nd_{0.5}Sr_{0.5}MnO_3$ has also been studied by Raman spectroscopy [25–28]. In particular, Asselin *et al* [28] have shown that the $Nd_{0.5}Sr_{0.5}MnO_3$ Raman active phonons

retrace the evolution between the paramagnetic, ferromagnetic, A-type antiferromagnetic and CE-type antiferromagnetic charge and orbital ordering phase transitions. To our knowledge there has been no published study of the $Nd_{0.5}Ca_{0.5}MnO_3$ Raman active phonons.

In this paper, with the Raman scattering technique constituting a very sensitive probe of local and dynamical changes, we present a study of $Nd_{0.5}Ca_{0.5}MnO_3$ Raman active modes under a microscope, focusing on $\sim$3 μm diameter areas. We have selected high quality single microcrystals free of twinning in order to verify the phonon associated selection rules and we have used the 632.8 nm (1.96 eV) He–Ne laser line so that the phonon intensities become resonantly enhanced as predicted around 1.9 eV [29]. Our objectives are (i) to determine whether the Raman active excitations reflect the evolution of the multiple phase transitions between room temperature and 20 K, (ii) to compare $Nd_{0.5}Ca_{0.5}MnO_3$ to the two systems $Nd_{0.5}Sr_{0.5}MnO_3$ and $La_{0.5}Ca_{0.5}MnO_3$, (iii) to detect whether phase separation develops at various temperatures as inferred from recent models [7, 22] and whether ferromagnetic fluctuations persist even below T_N as shown by NMR measurements for $La_{0.5}Ca_{0.5}MnO_3$ [30] with possible charge ordering occurring in the ferromagnetic regions [11, 31].

2. Experiments

The $Nd_{0.5}Ca_{0.5}MnO_3$ single crystals, typically platelike with (001) oriented faces ($\sim$1 mm, 2 mm, 200 μm), were grown by the floating zone method as described in [32]. 0.5 cm^{-1} resolution Raman spectra were measured in the backscattering configuration using a He–Ne laser (632.8 nm) and a Labram-800 Raman microscope spectrometer equipped with 50$\times$ objective, an appropriate notch filter and a nitrogen cooled CCD detector. The sample was mounted on the cold finger of a micro-helium Janis cryostat with the b direction or z axis ($Pnma$ symmetry) parallel to the incident radiation. The laser power was kept at 0.8 mW to avoid local heating. A_g and B_{2g} symmetry phonons were detected in the following configurations, using the Porto notation: $z(xx)\bar{z}$(A_g and B_{2g}), $z(x'x')\bar{z}$(A_g) and $z(x'y')\bar{z}$(B_{2g}); x, x' and y' stand for the [100], [110] and [$\bar{1}$10] quasicubic directions respectively. The absence of spurious signals was verified by the reproducibility of the spectra and their corresponding selection rules. Since twinnings occur unavoidably in platelike $Nd_{0.5}Ca_{0.5}MnO_3$, untwinned microcrystals within the sample were identified by using the Raman microscope in order to establish unambiguous Raman scattering selection rules. Such microcrystals were located when the A_g Raman active phonons obtained in the $(x'x')$ configuration became absent in the $(x'y')$ configuration in which only the B_{2g} signals are symmetry allowed. The sample was rotated until the incident laser beam polarization aligned with the x' axis so that pure A_g or B_{2g} symmetries were observed depending on the analyser orientation. With the incident polarization fixed, rotating further the sample by 45° permitted the setting of the xx and xy configurations.

The $Nd_{0.5}Ca_{0.5}MnO_3$ single-crystal dc magnetic susceptibility χ temperature dependence was measured using a vibration sample home-made magnetometer with the purpose of confirming the various magnetic phase evolutions. The susceptibility was determined via the measured magnetization in an $H = 10$ kOe magnetic field ($\chi = M/H$). The corresponding magnetization curves were linear with H over the whole temperature range. The heating and cooling regimes of the susceptibility measurements showed approximately similar results.

3. Results and discussion

Lowering the temperature from 300 K, the $Nd_{0.5}Ca_{0.5}MnO_3$ single-crystal dc susceptibility first increases, indicating the formation of a ferromagnetic phase (figure 1). The tendency towards ferromagnetism is opposed by charge ordering that favours antiferromagnetism and

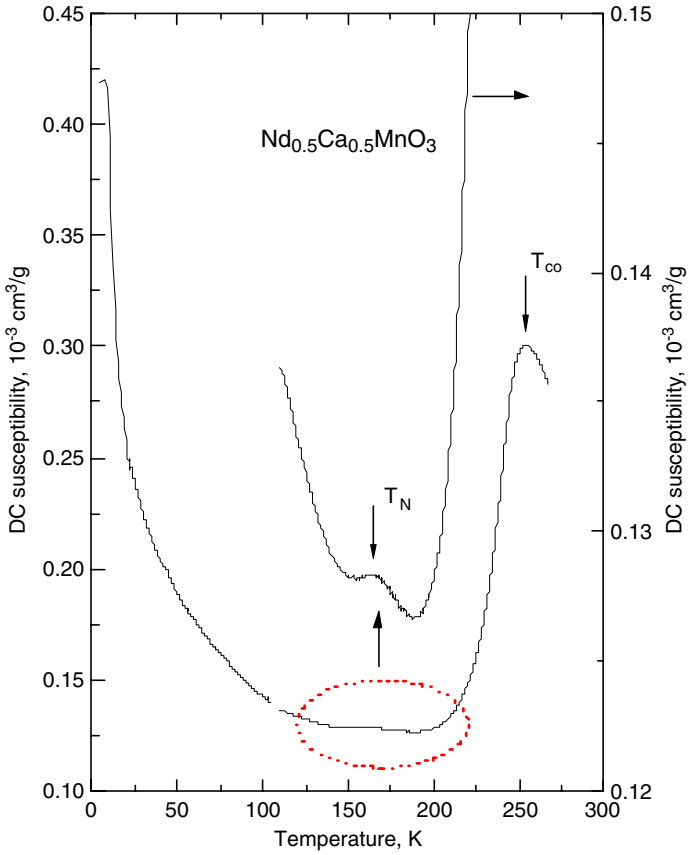

Figure 1. $Nd_{0.5}Ca_{0.5}MnO_3$ single-crystal dc susceptibility as a function of temperature. ↓ indicates the phase transitions due to charge ordering (T_{co}) and antiferromagnetic ordering (T_N). The weak anomaly at T_N is indicated by the enlargement with a right side scale (→).

(This figure is in colour only in the electronic version)

the peak that appears in the susceptibility at $T_{co} \sim 250$ K in figure 1 marks the quenching of the double-exchange interaction [33]. Below T_{co}, the susceptibility is reduced, suggesting the occurrence of short range order antiferromagnetic correlations and competition between ferromagnetic and antiferromagnetic interactions. Also the antiferromagnetic phase transition at $T_N \sim 160$ K is marked by a bump in the susceptibility as indicated by the enlargement in figure 1. Finally, at lower temperatures the susceptibility starts increasing, influenced by the Nd^{3+} ion ferromagnetic alignment.

For $Nd_{0.5}Ca_{0.5}MnO_3$, the Mn–O bonds present the most significant difference between room and low temperatures. While the oxygen octahedra are almost undistorted at room temperature with six approximately equal Mn–O bond lengths, the two Mn–O distances along the *b* axis become, below T_N, shorter than the four *a*–*c* plane Mn–O bonds, resulting in Jahn–Teller distortion [19].

In figures 2–4, $Nd_{0.5}Ca_{0.5}MnO_3$ Raman spectra at temperatures between 300 and 4.2 K are presented, for the xx (A_g and B_{2g}), $x'x'$ (A_g) and $x'y'$ (B_{2g}) configurations respectively. At 300 K, the $Nd_{0.5}Ca_{0.5}MnO_3$ space group is *Pnma* and three excitations at $\sim$265 cm^{-1} (A_g), 290 cm^{-1} (A_g) and 440 cm^{-1} (B_{2g}) are observed in the paramagnetic phase

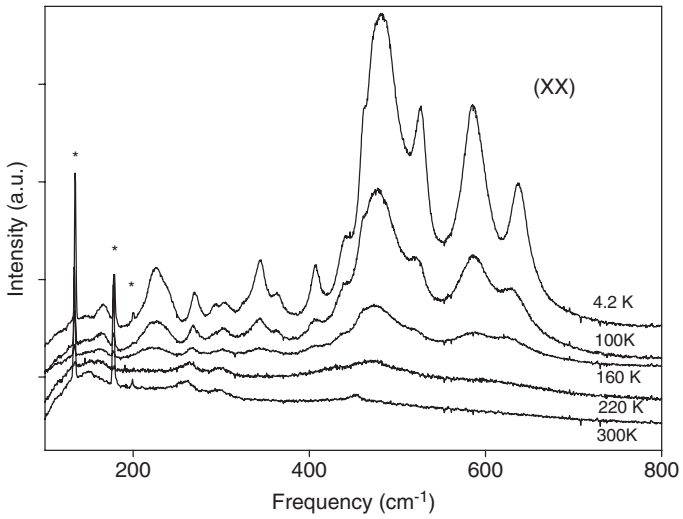

Figure 2. $Nd_{0.5}Ca_{0.5}MnO_3$ single-crystal Raman active phonons, in the xx scattering configuration, as a function of temperature. $*$ indicate plasma lines.

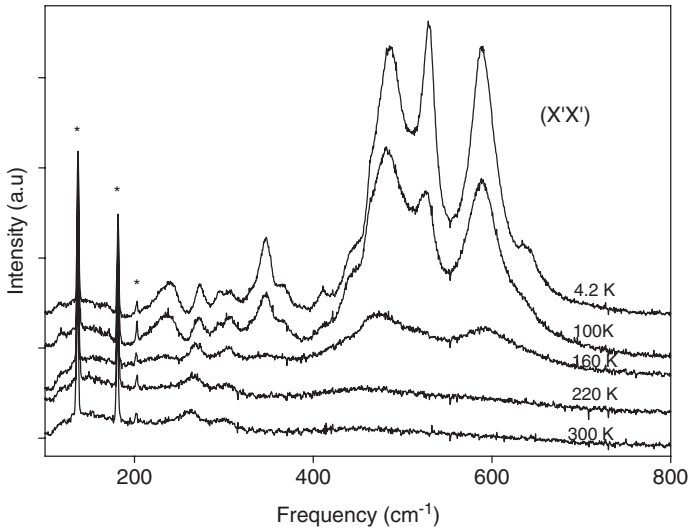

Figure 3. $Nd_{0.5}Ca_{0.5}MnO_3$ single-crystal Raman active phonons, in the $x'x'$. scattering configuration, as a function of temperature. $*$ indicate plasma lines.

where ferromagnetic correlations develop, while for $Nd_{0.5}Sr_{0.5}MnO_3$ and $La_{0.5}Ca_{0.5}MnO_3$ three bands centred at 205, 415 and 444 cm^{-1} [28] and at 230, 450 and 610 cm^{-1} [24] are detected respectively. Such bands have been associated with the insulating high temperature phase of the manganite rotation-like mode at ($\sim$250 cm^{-1}) which indicates the rotational and the Jahn–Teller ($\sim$450 cm^{-1}) distortions respectively [23]. On cooling the sample below $T_{co} \sim 250$ K, the space group remains $Pnma$ and new excitations develop at around 475 and 600 cm^{-1} delineating the charge order regime. Between T_{co} and T_N the unit cell volume shows a sharp variation ($\Delta V/V \approx 0.45\%$) and below T_N the structure adopts the monoclinic symmetry ($P2_1/m$) [20]. With the occurrence of the CE-type antiferromagnetism, many phonons become

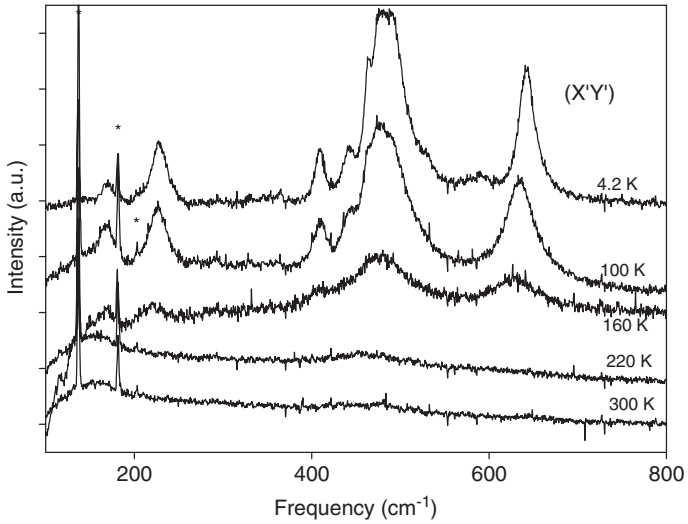

Figure 4. $Nd_{0.5}Ca_{0.5}MnO_3$ single-crystal Raman active phonons, in the $x'y'$ scattering configuration, as a function of temperature. $*$ indicate plasma lines.

Raman active and twenty excitations are observed (figures 2–4); their frequencies are compared to the corresponding excitations of $NdMnO_3$ [34], $CaMnO_3$ [35], $Nd_{0.5}Sr_{0.5}MnO_3$ [28] and $La_{0.5}Ca_{0.5}MnO_3$ [24] phonon frequencies in table 1.

The corresponding low symmetry monoclinic structure and the consequent large number of Raman allowed modes (54), as compared to the relatively small number of observed modes (20), hinder the symmetry analyses. Nevertheless, like $La_{0.5}Ca_{0.5}MnO_3$ [24] and $Nd_{0.5}Sr_{0.5}MnO_3$ [28], $Nd_{0.5}Ca_{0.5}MnO_3$ may be associated with a simplified *Pmma* structure characterized by charge and orbital ordering without octahedra tiltings. In such a structure nine external modes of stretching and bending types and twelve high frequency internal modes of translational and rotational types are predicted [24]. The Raman active modes may also be compared to the A_g and B_{2g} $NdMnO_3$ and $CaMnO_3$ (*Pnma* structure) Raman active phonons that involve mainly oxygen motions [34, 35]. The strongest $NdMnO_3$ and $CaMnO_3$ Raman active modes, 335 and 322 cm^{-1} (out-of-phase octahedral tilting), 482 and 465 cm^{-1} (octahedral basal oxygen out-of-phase stretching), 495 and 487 cm^{-1} (octahedral basal oxygen out-of-phase bending), respectively, and the $NdMnO_3$ 601 cm^{-1} (octahedral basal oxygen in-phase stretching) phonons are influenced by the temperature evolution of the Mn^{3+} ($NdMnO_3$) and Mn^{4+} ($CaMnO_3$) magnetic sublattices. They are observed in $Nd_{0.5}Ca_{0.5}MnO_3$ at 346, 479, 486 and 589 cm^{-1} respectively. In contrast to the 601 cm^{-1} $NdMnO_3$ phonon and the 487 and 465 cm^{-1} $CaMnO_3$ phonons which soften noticeably as temperature is lowered below the A-type antiferromagnetic transitions [34, 36], the $Nd_{0.5}Ca_{0.5}MnO_3$ 589, 486 and 479 cm^{-1} phonons do not soften and seem less affected by the CE-type antiferromagnetism. This underlines the sensitivity of the spin phonon coupling to the spin ordering in the xz plane as reflected by the phonon modulation of the nearest neighbour exchange interaction [37]. It seems that the A-type magnetic structures with ferromagnetic spin ordering in the xz planes that are coupled antiferromagnetically along the y axis are needed to provoke a significant phonon softening. In the CE-type structure, the spin ordering in the xz plane is somewhat complex. The charge and orbital ordering, allowing for both ferromagnetic and antiferromagnetic Mn^{3+}–Mn^{4+} interactions which form right angle couplings [38], do not favour phonon softening.

Table 1. Raman active phonon frequencies, in cm^{-1} at $T < T_N$, in $Nd_{0.5}Ca_{0.5}MnO_3$ (this work) as compared to $NdMnO_3$, $CaMnO_3$, $Nd_{0.5}Sr_{0.5}MnO_3$ and $La_{0.5}Ca_{0.5}MnO_3$ (published data). $\Delta\nu$ corresponds to the frequency hardening between 160 and 4.2 K.

$CaMnO_3$ [35]	$NdMnO_3$ [34]	$La_{0,5}Ca_{0,5}MnO_3$ [24]	$Nd_{0,5}Sr_{0,5}MnO_3$ [28]	$Nd_{0.5}Ca_{0.5}MnO_3$ This work
A_g	A_g	A_g	A_g	A_g $\Delta\nu$
			82	116 (2)
243	245	233	214(s)	239s (7)
278				274* (6)
				295* (1)
322		319	316	307 (0)
				331 (0)
	335(s)	337(s)	337 (s)	346s (0)
		359	358	367 (0)
	468		458	
487(s)	495(s)	487(s)	489(s)	486s (13)
		516(s)	509(s)	529s (5)
			543	
		601(s)	610(s)	589s (0)
				634
B_{2g}	B_{2g}	B_{2g}	B_{2g}	B_{2g}
				169 (0)
		217(s)	216(s)	227s (7)
258(s)		270	258	
	314			
		401	401	410 (0)
		429	428	443 (13)
	453			464s (0)
465(s)	482(s)	473	475(s)	479s (4)
	500			490s (4)
	601(s)			
		643	651(s)	643s (14)

The 645 cm^{-1} density of states infrared and Raman active excitations in $NdMnO_3$ which play an important role in the multiphonon processes [39], as well as the 245, 453 and 500 cm^{-1} phonons, are also present in $Nd_{0.5}Ca_{0.5}MnO_3$ at 643 cm^{-1}, 239, 464 and 490 cm^{-1} respectively. In addition to the $NdMnO_3$ phonons, the 319, 359, 516 cm^{-1} A_g and 217, 401, 429 cm^{-1} B_{2g} $La_{0.5}Ca_{0.5}MnO_3$ phonons, whose vibrational pattern has been described in [24], have their counterparts in $Nd_{0.5}Ca_{0.5}MnO_3$ at 307, 367, 529 cm^{-1} A_g and 227, 410, 443 cm^{-1} B_{2g} phonons respectively. Finally, two additional phonons at 116 cm^{-1} (A_g) and 169 cm^{-1} (B_{2g}) are also observed in $Nd_{0.5}Ca_{0.5}MnO_3$.

Between room temperature and T_N, the three excitations observed in the ferromagnetic regime followed by the two excitations in the charge order at T_{co} are possibly induced by dynamical incoherent Jahn–Teller distortions [40]. No broad band similar to the 205 cm^{-1} room temperature excitation in $Nd_{0.5}Sr_{0.5}MnO_3$ has been observed in $Nd_{0.5}Ca_{0.5}MnO_3$. Such excitation has been associated with the soft mode observed in rhombohedral $LaMnO_3$ [41] and $La_{1-x}Sr_xMnO_3$ [42] indicating possible occurrence of rhombohedral distortions in $Nd_{0.5}Sr_{0.5}MnO_3$, absent for $Nd_{0.5}Ca_{0.5}MnO_3$.

Similarly to the $Nd_{0.5}Sr_{0.5}MnO_3$ case, the high temperature phase phonons of $Nd_{0.5}Ca_{0.5}MnO_3$ persist below T_N indicating the occurrence of phase separation at low

temperature and confirming a previous NMR study of $La_{0.5}Ca_{0.5}MnO_3$ [30]. The observation of the room temperature phonons below T_N is also consistent with the Brillouin scattering study [21] which is, in contrast to an ESR study [43], strongly indicative of the presence of ferromagnetic inhomogeneities in the charge ordered as well as antiferromagnetic phases [21]. It would also confirm the assertion that charge order could occur in ferromagnetic regions [11] if the ferromagnetic regime phonons, above T_{co}, reflect distortions due to some charge ordering.

At $T_{co} < T < T_N$ phonon excitations around the 475 and 600 cm^{-1} bending and stretching bands are broad and disorder induced, indicating spatially incoherent Jahn–Teller distortions. Below T_N, with charge and complete orbital orderings, these excitations strengthen and sharpen becoming Raman allowed following the occurrence of static and coherent Jahn–Teller distortions. In the CE-type antiferromagnetic phase many additional Raman excitations are strongly intensity enhanced as temperature is lowered. They are compatible with charge and orbital orderings as in $Nd_{0.5}Sr_{0.5}MnO_3$ and $La_{0.5}Ca_{0.5}MnO_3$, delineating the sample structural evolutions. Group theory predicts 63 infrared active modes in the monoclinic CE-type phase [24]. Nevertheless, the numerous $Nd_{0.5}Ca_{0.5}MnO_3$ Raman active modes observed in the CE-type phase (20 modes) are in contrast with the reported infrared absorption measurements where four broad absorption bands associated with stretching ($\sim$600 cm^{-1}), bending ($\sim$360 and 400 cm^{-1}) and lattice ($\sim$200 cm^{-1}) modes are detected at room temperature and only one additional stretching mode ($\sim$520 cm^{-1}) is observed below T_N [44].

Interestingly, many phonons in the charge and orbital ordered phase harden significantly between 160 and 4.2 K ($\Delta\nu$ of table 1). These phonons, with dominant oxygen motions in the xz plane, particularly the A_g 486 cm^{-1} (rotation) and the B_{2g} 643 cm^{-1} (stretching) [24], would reflect the e_g orbital ordering effects and resultant changes in the Mn–O bond covalency. Similar noticeable phonon hardening in the charge–orbital ordered state of the layered manganites $La_{0.5}Sr_{1.5}MnO_4$ and $LaSr_2Mn_2O_7$ has been reported [45].

In $R_{1-x}A_xMnO_3$ (e.g. $Nd_{0.5}Sr_{0.5}MnO_3$, $Nd_{0.5}Ca_{0.5}MnO_3$) the average radius of the A-site cations $\langle r_A \rangle$ (1.24 Å, 1.17 Å) influences T_{co} (150, 250 K), the Mn–O–Mn angle (165°, 157°) and the average Mn–O bond length (1.927, 1.945 Å) [46]. Such parameters would affect the phonon frequencies of a given mode and account for the observed frequency differences in similar compounds such as $Nd_{0.5}Sr_{0.5}MnO_3$ and $Nd_{0.5}Ca_{0.5}MnO_3$.

Also as $\langle r_A \rangle$ decreases, the MnO_6 tilting increases [9] and enhances the corresponding mode frequency by $\sim$9 cm^{-1} (337 cm^{-1} in $Nd_{0.5}Sr_{0.5}MnO_3$ as compared to 346 cm^{-1} in $Nd_{0.5}Ca_{0.5}MnO_3$).

The overall strong similarities in the $Nd_{0.5}Sr_{0.5}MnO_3$, $Nd_{0.5}Ca_{0.5}MnO_3$ and $La_{0.5}Ca_{0.5}MnO_3$ CE-type phase Raman active phonons are indicative of the universal character of charge and orbital ordering in the manganites. The Raman spectroscopy successfully reflects such ordering and locally probes their temperature evolutions in the detected phonon intensities and frequencies.

4. Conclusion

A resonant Raman study of $Nd_{0.5}Ca_{0.5}MnO_3$ untwinned microcrystals has allowed the detection of three phonons between $T = 300$ K and T_{co} and two additional phonons between T_{co} and T_N. At $T < T_N$, the CE-type phase dominates and, in contrast to the previously small number of infrared active modes detected, twenty Raman active modes have been detected and compared to $NdMnO_3$ [34], $CaMnO_3$ [35], $Nd_{0.5}Sr_{0.5}MnO_3$ [28] and $La_{0.5}Ca_{0.5}MnO_3$ [24] low temperature phonon frequencies. The persistence of high temperature ferromagnetic and A-type antiferromagnetic phase phonons corroborates the phase separation development. In addition to the $La_{0.5}Ca_{0.5}MnO_3$, $Nd_{0.5}Sr_{0.5}MnO_3$ and $Nd_{0.5}Ca_{0.5}MnO_3$ crystalline structures

being identical, the phonon symmetries and MnO_6 octahedra stretching, bending and tilting frequencies in the CE-type phase indicate coherent cooperative Jahn–Teller distortions as well as strong similarities of the Ca and Sr doped manganite charge and orbital orders.

Acknowledgments

S Jandl acknowledges support from the National Science and Engineering Research Council of Canada, and the Fonds Québécois de la Recherche sur la Nature et les Technologies. This work was supported in part by the Russian Foundation for Basic Research (03-02-16759) and the Quantum Macrophysics Programme of the Russian Academy of Sciences.

References

[1] Zener C 1951 *Phys. Rev.* **82** 403
[2] Jim S, Tiefel T H, McCormack M, Fastnacht R, Ramesh R and Chen L H 1994 *Science* **264** 413
[3] Khomskii D I and Sawatzky G A 1997 *Solid State Commun.* **102** 87
[4] Woodward P M, Vogt T, Cox D E, Arulraj A, Rao C N R, Karen P and Cheetham A K 1998 *Chem. Mater.* **10** 3652
[5] Coey J M D, Viret M and von Molnar S 1999 *Adv. Phys.* **48** 167
[6] Uehara M, Mori S, Chen C H and Cheong S W 1999 *Nature* **399** 560
[7] Dagotto E, Burgy J and Moreo A 2003 *Solid State Commun.* **126** 9
[8] Salamon M B and Jaime M 2001 *Rev. Mod. Phys.* **73** 583
[9] Rao C N R, Arulraj A, Cheetham A K and Raveau B 2000 *J. Phys.: Condens. Matter* **12** R83
[10] Radaelli P G, Cox D E, Marezio M and Cheong S W 1997 *Phys. Rev.* B **55** 3015
[11] Loudon J C, Mathur N D and Midgley P A 2002 *Nature* **420** 797
[12] Caignaert V, Millange F, Hervieu M, Suard E and Raveau B 1996 *Solid State Commun.* **99** 173
[13] Tokunaga M, Miura N, Tomioka Y and Tokura Y 1998 *Phys. Rev.* B **57** 5259
[14] Ramirez A P 1997 *J. Phys.: Condens. Matter* **9** 8171
[15] Popov Y F, Kadomtseva A M, Vorob'ev G P, Kamilov K I, Shotfich Y S, Ivanov V Y, Mukhin A A and Balbashov A M 2003 *Phys. Status Solidi* **45** 1280
[16] Popov Y F, Kadomtseva A M, Vorob'ev G P, Kamilov K I, Mukhin A A, Ivanov V Yu and Balashov A M 2004 *Phys. Status Solidi* **46** 2222
[17] Kuwahara H, Tomioka Y, Asamitsu A, Moritimo Y and Tokura Y 1995 *Phys. Rev. Lett.* **74** 5108
[18] Pollert E, Krupicka S and Kuzmicova E 1982 *J. Phys. Chem. Solids* **43** 1137
[19] Millange F, de Brion S and Chouteau G 2000 *Phys. Rev.* B **62** 5619
[20] Vogt T, Cheetham A K, Mahendiran R, Raychaudhuri A K, Mahesh R and Rao C N R 1996 *Phys. Rev.* B **54** 15303
[21] Murugavel P, Narayana C, Sood A K, Parashar S, Raju A R and Rao C N R 2000 *Europhys. Lett.* **52** 461
[22] Mayr M, Moreo J A, Vergés J A, Arispe J, Feiguin A and Dagotto E 2001 *Phys. Rev. Lett.* **86** 135
[23] Iliev M N, Abrashev M V, Popov V N and Hadjiev V G 2003 *Phys. Rev.* B **67** 212301
[24] Abrashev M V, Bäckström J, Börjesson L, Pissas M, Kolev N and Iliev M N 2001 *Phys. Rev.* B **64** 144429
[25] Kuroe H, Habu I, Kuwahara H and Sekine T 2002 *Physica* B **316/317** 575
[26] Choi K Y, Lemmens P, Güntherodt G, Pattabiraman M, Rangarajan G, Gnezdilov V P, Balakrishnan G, Paul D M^c K and Lees M R 2003 *J. Phys.: Condens. Matter* **15** 3333
[27] Seikh M M, Sood A K and Narayana C 2005 *Pramana* **64** 119
[28] Asselin A, Jandl S, Fournier P, Mukhin A A, Ivanov V Yu and Balbashov A M 2005 *J. Phys.: Condens. Matter* **17** 5247
[29] Allen P B and Perebeinos V 1999 *Phys. Rev. Lett.* **83** 4828
[30] Allodi G, De Renzi R, Licci F and Pieper M W 1998 *Phys. Rev. Lett.* **81** 4736
[31] Mori S, Chen C H and Cheong S W 1998 *Phys. Rev. Lett.* **81** 3972
[32] Balbashov A M, Karabashev S G, Mukovskiy Ya M and Zverkov S A 1996 *J. Cryst. Growth* **167** 365
[33] Pollert E, Krupicka S and Kuzmicova E 1982 *J. Phys. Chem. Solids* **43** 1137
[34] Jandl S, Barilo S N, Shiryaev S V, Mukhin A A, Ivanov V Yu and Balbashov A M 2003 *J. Magn. Magn. Mater.* **264** 36

[35] Abrashev M V, Bäckström J, Börjesson L, Popov V N, Chakalov R A, Kolev N, Meng R L and Iliev M N 2002 *Phys. Rev.* B **65** 18430
[36] Granado E, Moreno N O, Martinho H, Garcia A, Sanjurjo J A, Torriani I, Rettori C, Neumier J J and Oseroff S B 2001 *Phys. Rev. Lett.* **86** 5385
[37] Granado E, Garcia A, Sanjurjo J A, Rettori C, Torriani I, Prado F, Sanchez R D, Canairo A and Oseroff S B 1999 *Phys. Rev.* B **60** 11879
[38] Radaelli P G, Cox D E, Marezio M and Cheong S W 1997 *Phys. Rev.* B **55** 3015
[39] Jandl S, Mukhin A A, Ivanov V Yu and Balbashov A M 2006 *Physica* B submitted
[40] Iliev M N and Abrashev M V 2001 *J. Raman Spectrosc.* **32** 805
[41] Abrashev M V, Litvinchuk A P, Iliev M N, Meng R L, Popov V N, Ivanov V G, Chakalov R A and Thomsen C 1999 *Phys. Rev.* B **59** 4146
[42] Podobedov V B, Weber A, Romero D B, Rice J P and Drew H D 1998 *Solid State Commun.* **105** 589
[43] Dupont F, Millange F, De Brion S, Janossy A and Chouteau G 2001 *Phys. Rev.* B **64** 220403
[44] Arulraj A and Rao C N R 1999 *J. Solid State Chem.* **145** 557
[45] Yamamoto K, Kimura T, Ishikawa T, Katsufuji T and Tokura Y 2000 *Phys. Rev.* B **61** 14706
[46] Arulraj A, Santosh P N, Srinivasa G R, Guha A, Raychaudhuri A K, Kumar N and Rao C N R 1998 *J. Phys.: Condens. Matter* **10** 8497